Salmosan®, a β-galactomannan-rich product, protects epithelial barrier function in Caco-2 cells infected by *Salmonella enterica* serovar Enteritidis[1-4]

M Teresa Brufau[4], Joan Campo-Sabariz[4], Ricard Bou[5], Sergi Carné[6], Joaquim Brufau[7], Borja Vilà[7], Ana M Marqués[8], Francesc Guardiola[5], Ruth Ferrer[4], Raquel Martín-Venegas[4*]

[4]Departament de Fisiologia, Facultat de Farmàcia, Universitat de Barcelona, Barcelona; [5]Departament de Nutrició i Bromatologia, Facultat de Farmàcia, Universitat de Barcelona, Barcelona; [6]Industrial Técnica Pecuaria S.A. (ITPSA), Barcelona; [7]Institut de Recerca i Tecnologia Agroalimentàries, Nutrició Benestar Animal, Constantí; and [8]Departament de Microbiologia i Parasitologia Sanitàries, Facultat de Farmàcia, Universitat de Barcelona, Barcelona

***Corresponding author:**

Department de Fisiologia, Facultat de Farmàcia, Universitat de Barcelona, Av. Joan XXIII s/n, E-08028 Barcelona.

Telephone number: +34 934024505

Fax number: +34 934035901

raquelmartin@ub.edu

CITATION: M Teresa Brufau, Joan Campo-Sabariz, Ricard Bou, Sergi Carné, Joaquim Brufau, Borja Vilà, Ana M Marqués, Francesc Guardiola, Ruth Ferrer, Raquel Martín-Venegas, Salmosan, a β-Galactomannan-Rich Product, Protects Epithelial Barrier Function in Caco-2 Cells Infected by *Salmonella enterica* Serovar Enteritidis, *The*

Journal of Nutrition, Volume 146, Issue 8, August 2016, Pages 1492–1498, https://doi.org/10.3945/jn.116.232546

Running title: Effect of β-galactomannans on Caco-2 cells

[1]Abbreviations: DCFH, 2',7'-dichlorofluorescein; DPBS, *Dulbecco's* PBS; FD-4, fluorescein isothiocyanate–dextran; LDH, lactate dehydrogenase; MOI, multiplicity of infection; MOS, mannan oligosaccharides; PP, Paracellular permeability; ROS, Reactive oxygen species; S-βGM, Salmosan®; TER, transepithelial electrical resistance; TJ, tight junction; TSA, Tryptic soy agar; ZO-1, zonula occludens protein-1.

[2]Financial support: This work was supported by project FRI-2011 of the *Institut de Recerca en Nutrició i Seguretat Alimentària* (INSA-UB) and by ITPSA.

[3]Conflict of interest and funding disclosure: J. Brufau is one of the inventors of patent S-βGM WO2009/144070 A2, which is commercially licensed to ITPSA. This fact did not alter the author's adherence to all the Journal of Nutrition policies on data collection and analysis, preparation of the manuscript, or sharing data and materials. The other authors declare that they have no competing interests.

[4]Supplemental Figure 1 and Supplemental Figure 2 are available from the "Online Supporting Material" link in the online posting of the article and from the same link in the online table of contents at http://jn.nutrition.org

Abstract

Background: One promising strategy for reducing human salmonellosis induced by *Salmonella* Enteritidis is to supplement animal diets with natural feed additives such as mannan oligosaccharides (MOS).

Objective: The aim of this study was to investigate the potential role of Salmosan® (S-βGM), an extremely β-galactomannan-rich MOS product, in preventing epithelial barrier function disruption induced by *Salmonella* Enteritidis colonization in an *in vitro* model of intestinal Caco-2 cells in culture.

Methods: Differentiated Caco-2 cells were incubated for 3 h with *Salmonella* Enteritidis at a multiplicity of infection 10 (MOI 10) in the absence or presence of 500 µg/mL S-βGM. Paracellular permeability (PP) was assessed by transepithelial electrical resistance (TER), D-mannitol and fluorescein isothiocyanate–dextran (FD-4) flux. Tight junction (TJ) proteins and cytoskeletal actin were also localized by confocal microscopy. Reactive oxygen species (ROS) and lipid peroxidation products were evaluated. Scanning and transmission electron microscopy were used to visualize *Salmonella* Enteritidis adhesion to, and invasion of, the Caco-2 cell cultures.

Results: Compared to controls, TER was significantly reduced 30 %, and D-mannitol and FD-4 flux were significantly increased 374 % and 54 % in *Salmonella* Enteritidis-infected cultures. The presence of S-βGM in infected cultures induced total recoveries of TER and FD-4 flux to values that did not differ from control ($P = 0.07$ and $P = 0.55$, respectively), and a partial recovery of D-mannitol flux. These effects were confirmed by immunolocalization of actin, zonula occludens protein-1 (ZO-1) and occludin. Similar results were obtained for *Salmonella* Dublin. The protection of S-βGM on PP in infected cultures may be associated with a total recovery of ROS production to values that did not differ from control ($P = 0.11$). Moreover, S-βGM has the capacity to

agglutinate bacteria, leading to a significant reduction in intracellular *Salmonella* Enteritidis of 32 % ($P < 0.05$).

Conclusions: The results demonstrate that S-βGM contributes to protecting epithelial barrier function in a Caco-2 cell model disrupted by *Salmonella* Enteritidis.

Key words: *Salmonella* Dublin, paracellular permeability, tight junction, TER, FD-4, D-mannitol, occludin, ZO-1, actin, ROS

Introduction

Salmonella Enteritidis is one of the leading causes of food-borne salmonellosis in humans worldwide. It is associated with the consumption of contaminated food of animal origin, mainly poultry and eggs (1-5). In chickens, young birds are more susceptible to *Salmonella* Enteritidis infection and to developing systemic disease with varying degrees of mortality, whereas most adult animals typically remain asymptomatic and thus become an important source of infection (6-8).

Salmonella possesses mannose-specific lectins in type-1 fimbriae that adhere to glycoproteins in the intestinal epithelium (9) and allow passage through enterocytes and microfold (M) cells (10). Uptake into non-phagocytic cells is facilitated by virulence proteins delivered into the host cell cytoplasm by type III secretion system 1 (T3SS-1). Activation of T3SS-1 induces cytoskeletal rearrangements, bacterial internalization due to the formation of lamellipodia, and nuclear reactions leading to the production of proinflammatory cytokines (11).

Recent findings indicate that *Salmonella* can also disrupt intercellular junctions, increasing paracellular permeability (PP) and transepithelial bacterial translocation, thus

facilitating its pathogenicity (12, 13). Tight junctions (TJs), the most apical and rate-limiting step for PP, are composed of transmembrane proteins, such as claudins and occludin, and different cytosolic proteins [zonula occludens protein-1 (ZO-1), 2, 3, AF6 and cingulin] which form the nexus of transmembrane proteins with the cytoskeleton, mainly with the perijunctional ring of actomyosin (14, 15).

The use of antibiotic growth promoters (AGP) in animal feed is prohibited in the European Union due to the risk of developing resistance to antibiotics in human consumers (regulation [EC] no. 1831/2003). However, natural feed additives such as mannan oligosaccharides (MOS) are promising alternatives to AGP (16). MOS are natural substances present in plants and in the wall of the yeast *Saccharomyces cerevisiae* var. Boulardii, and have prebiotic properties (9, 17, 18). It has been reported that MOS benefit the intestinal function by improving gut health (19) and enhancing innate immune responses (16, 20). In addition, diverse bacterial strains other than *Salmonella* may adhere to MOS by mannose-specific lectins in type 1 fimbriae, thus competing for bacterial adhesion to glycoproteins in the intestinal epithelium, also rich in mannose, and preventing intestinal infection (9, 21). In a previous study, we found that dietary supplementation with β-galactomannans in chickens infected with *Salmonella* Enteritidis increases villus length, and thus epithelial surface area, and mucus production, an effect associated with improved intestinal barrier function (22).

In light of the above, the aim of this study was to investigate the potential role of Salmosan® (S-βGM), a hydrolyzed MOS highly β-galactomannan-rich product developed from the carob bean of the *Ceratonia siliqua* tree and guar bean of the *Cyamopsis tetragonoloba*, in preventing epithelial barrier function disruption induced

by *Salmonella* Enteritidis colonization in an *in vitro* model of intestinal Caco-2 cells. Since oxidative stress is considered one of the main factors involved in epithelial barrier function disruption (23), we also investigated the protective effect of S-βGM on the production of intracellular reactive oxygen species (ROS) and on lipid peroxidation. Moreover, given that *Salmonella* serovars may differ significantly in their human pathogenic potential, we also studied the capacity of S-βGM to protect cultures infected by *Salmonella* Dublin, which is present in cattle intestine and is more invasive and has a more severe clinical course in humans than *Salmonella* Enteritidis (24).

Material and methods

Material

DMEM, trypsin, penicillin and streptomycin were supplied by GIBCO (Paisley, Scotland). *Dulbecco's* PBS (DPBS), HEPES, fluorescein isothiocyanate–dextran (FD-4, average mol wt 3,000–5,000), genistein, H_2O_2, EDTA and other chemicals were purchased from Sigma-Aldrich (St. Louis, MO, USA). Tryptic soy agar (TSA) was purchased from Thermo Fisher Scientific Oxoid (Hampshire, UK). Tissue culture supplies, including Transwells, were obtained from Costar (Cambridge, MA, USA). Cyclohexane (spectrophotometric grade), chloroform and methanol were purchased from Panreac (Barcelona, Spain). Paraformaldehyde was purchased from Aname (Barcelona, Spain). D-[2-^{3}H]-mannitol (specific activity 30 Ci/mmol) was purchased from American Radiolabeled Chemicals Inc. (St. Louis, MO). S-βGM was kindly provided by Industrial Técnica Pecuaria (ITPSA, Barcelona, Spain).

Bacterial growth

Pathogenic *Salmonella* Enteritidis (phage type 4, nalidixic acid-resistant strain) and *Salmonella* Dublin were provided by Dr. Ignacio Badiola from the *Centre de Recerca en Sanitat Animal* (CReSA, IRTA-UAB, Bellaterra, Spain). To prepare the *Salmonella* inoculum (NaCl, 9 g/L), the bacteria were grown at 37°C in TSA for 24 h and used in the exponential growth phase as determined by absorbance at 600 nm.

Cell culture

Caco-2 cells were provided by the American Type Culture Collection and were cultured as previously described (25). Cells (passage 63-80) were subcultured at a density of 10^5 cells/cm^2 on polycarbonate filters (Transwells) for PP experiments, TJ protein immunolocalization and transmission electron microscopy; at a density of 10^4 cells/cm^2 on 12-well clusters for intracellular ROS determination, bacterial adhesion capacity and invasion assay; in 150 cm^2 flasks for evaluation of lipid peroxidation; and on poly-L-lysine coated glass coverslips in Petri dishes for scanning electron microscopy.

Infection of Caco-2 with *Salmonella* Enteritidis and *Salmonella* Dublin

The monolayers were washed twice and stabilized with DMEM without antibiotics for 2 h at 37°C in 5% CO_2. The cells were then incubated for 3 h with *Salmonella* Enteritidis or Dublin in the apical compartment at a multiplicity of infection (MOI) of 3-50. The same volume of saline solution was added to the monolayers that were not infected (Control cells). Caco-2 cell viability was assessed from lactate dehydrogenase (LDH) activity in the apical medium at the end of the incubation period with the bacterium, following the manufacturer's instructions (TECAN, Sunrise, Grödig, Austria).

S-βGM preparation

S-βGM (patent WO2009/144070 A2, licensed to ITPSA) consists of a β-(1-4)-mannose backbone with branched galactose molecules (galactose:mannose ratio of 1:4) plus β-mannanase. For the experiments, S-βGM was diluted in DMEM without antibiotics (10-1000 µg/mL), vortexed and incubated for 30 min at 37ºC, and then added to the apical side of the monolayers 30 min prior to incubation with the bacterium.

Paracellular permeability

PP was estimated from transepithelial electrical resistance (TER) and transepithelial D-mannitol and fluorescein isothiocyanate–dextran (FD-4) fluxes. For FD-4 flux, 9 mg/mL of FD-4 was added to the apical side of the monolayer two hours after incubation with *Salmonella*, and at the end of the experiment, the amount of FD-4 was quantified in an aliquot of the basolateral compartment by fluorimetry (Wallac 1420 Victor3 fluorometer, Perkin-Elmer, Waltham, MA) at excitation and emission wavelengths of 480 nm and 535 nm respectively. TER and D-mannitol flux were determined after 3 h incubation with *Salmonella* as described elsewhere (25). The addition of 300 µM genistein to the apical side of the monolayer during *Salmonella* incubation was also tested.

Confocal immunolocalization

At the end of the incubation period with the bacterium, Caco-2 monolayers were immune-stained as described elsewhere (25). Mouse monoclonal anti-occludin (1:250 dilution; Life Technologies) and rabbit polyclonal anti-ZO-1 (1:250 dilution; Life Technologies) were used as primary antibodies. Alexa dye-conjugated secondary antibodies (1:300 dilution; Alexa Fluor 647 and 488, respectively, Life Technologies) and phalloidin-tetramethylrhodamine B isothiocyanate to view the cytoskeletal

subapical actin ring (1:500 dilution; Sigma-Aldrich) were used. Finally, cells were examined with a confocal laser scanning microscope (TCS-SP5; Leica Lasertechnik, GmbH, Germany). Images were taken using a 63x (numerical aperture 1.3, phase 3, oil) Leitz Plan-Apochromatic objective and processed by ImageJ software (public domain, National Institutes of Health) to quantify fluorescence in horizontal planes of the monolayer as described by Martín-Venegas et al. (26).

Intracellular reactive oxygen species (ROS)

Intracellular ROS generation was evaluated by intracellular oxidation of 2',7'-dichlorofluorescein (DCFH) to the fluorescent compound dichlorofluorescein (DCF), performed using a commercial intracellular ROS assay kit (OxiSelect™, Cell Biolabs Inc., Bionova, Barcelona) following the manufacturer's instructions. Prior to inoculation with *Salmonella,* Caco-2 monolayers were washed with DPBS and incubated at 37°C with DCFH (100 µmol/L in DMEM) for 40 min in attenuated light conditions. The monolayers were then washed twice with DMEM without antibiotics to ensure the removal of all unloaded indicator. At the beginning and end of the incubation period, the intensity of fluorescence was measured (Wallac 1420 Victor3, Perkin-Elmer, Waltham, MA) at excitation and emission wavelengths of 480 nm and 535 nm, respectively.

Lipid peroxidation

Lipid ultraviolet absorption was used to monitor the formation of lipid oxidation products measuring absorbance at 235 nm (mainly attributable to conjugated dienes) and 270 nm (mainly attributable to secondary oxidation products). At the end of the incubation period with the bacterium, Caco-2 cell cultures were trypsinized and 200 mg

of pelleted cells was suspended in 1 mL of 0.1% EDTA. The suspension was mixed with 6 mL chloroform-methanol (2:1) and homogenized (Polytron®, Kinematica, Luzern, Switzerland) and the extracted lipid fraction was then decanted and reserved. The suspension was extracted again with 6 mL of chloroform-methanol (2:1) and homogenized, and this second lipid fraction was then decanted together with the first one. The extracted lipid fraction was diluted with 4 mL of milliQ water and centrifuged (400 *g*, 20 min). The chloroform phase was filtered through anhydrous sodium sulfate (Whatman number 1), which was washed twice with 5 mL of chloroform. The lipid extract thus obtained was concentrated to 1 mL in a vacuum rotatory evaporator at 35ºC and the rest of the solvent was removed first bay a slight nitrogen stream, and then by keeping the flask in a vacuum desiccator at 10 mm Hg for 2 h. The organic solvent was removed under a rotary evaporator and nitrogen stream. The extracted lipid fraction was then dissolved in 2 mL of cyclohexane, and absorbance was determined in a double-beam spectrophotometer (Shimadzu UV-160A, Japan) at 235 nm and 270 nm. The spectrophotometric conditions were as follows: spectrum range 200-300 nm and 1 cm quartz cuvettes.

Scanning and transmission electron microscopy

For scanning electron microscopy, the cells were processed after the incubation period as previously described (21), except that cells were fixed in 2.5% paraformaldehyde in PBS (0.1 M, pH 7.4). The samples were examined in a Zeiss DSM 940A (Oberkochen, Germany) microscope operating at 15 kV. For transmission electron microscopy, the cells were prepared as previously described (27) and observed in a JEOL JEM 1010 microscope (Tokyo, Japan) operating at 80 kV.

Cell-associated bacterial experiment

To evaluate *Salmonella* invasion, at the end of the incubation period of Caco-2 cells with the bacterium, monolayers were washed and incubated for an additional 1 h with DMEM containing 100 U/mL penicillin and 100 µg/mL streptomycin at 37°C to kill residual adhered extracellular bacteria. After treatment with antibiotics, the monolayers were washed three times with DPBS and lysed by addition of 0.5% Triton-X100 in DPBS. The resulting suspension was serially diluted in DPBS and plated onto TSA at 37°C for 24 h. To investigate *Salmonella* adhesion, considered as *Salmonella* adhered to the epithelium plus invasion, the same protocol was followed except that incubation with antibiotics was omitted. The effect of S-βGM on *Salmonella* viability was investigated in a bacterial suspension in DMEM with the same bacterial concentration as in Caco-2 cell culture experiments. The suspension was incubated for 3 h at 37°C in the absence or presence of S-βGM, and at the end of the incubation period, a sample of the suspension was serially diluted in DPBS and plated onto TSA at 37°C for 24 h.

Statistical analysis

Data were analyzed by 1-way ANOVA followed by Bonferroni's or Dunnett's post hoc tests, or Student's t test using SPSS® software (SPSS Inc. Chicago, IL). $P < 0.05$ was considered to denote statistical significance.

Results

To establish the experimental conditions, a MOI of 10 was chosen since this is the lowest infection ratio that induced a significant effect on TER and D-mannitol flux (**Figure 1**) without affecting LDH activity (data not shown).

The protective effect of S-βGM in *Salmonella* Enteritidis infection was tested for 4 product concentrations: 10, 100, and 500 μg/mL and 1 mg/mL (data not shown). Of these, 500 μg/mL was the lowest concentration that showed a protective effect on both TER (**Figure 2A**) and D-mannitol flux (**Figure 2B**), and no differences were detected with respect to the highest concentration tested (P = 0.12 and P = 0.06 for TER and D-mannitol flux, respectively). While protection was complete for TER (P = 0.07 respect to Control), D-mannitol flux did not attain Control values. When FD-4 flux were investigated (**Figure 2C**), the results showed a lower effect for *Salmonella* infection (MOI of 10; 1.6-fold increase for FD-4 flux compared to 4.8-fold increase for D-mannitol flux) and a complete protective effect for 500 μg/mL S-βGM (P = 0.55 respect to Control). The results also showed that genistein, a tyrosine kinase inhibitor (28), partially prevented changes in D-mannitol flux, whereas totally recovery was seen in TER values (P = 0.05 respect to Control).

In Control cultures, occludin, ZO-1 and subapical actin ring were visualized delineating the cellular borders (**Figure 3A**). In cultures infected with *Salmonella* Enteritidis, the images revealed that the three proteins showed a reduction in fluorescence and lost their outline, and these results were confirmed by fluorescence quantification in these images (**Figure 3B**). The images also revealed the appearance of diffuse cytoplasmic occludin accumulations. In the case of actin, stellate focal points of fluorescence were observed in the convergence of several cells (Figure 3A). Incubation with S-βGM led to the recovery of fluorescence (Figure 3A and B) for ZO-1 and actin, although stellate actin accumulations did not disappear. As for occludin, the images revealed the presence of abundant cytoplasmic accumulations.

Infection with *Salmonella* Enteritidis significantly increased ROS production, which was completely prevented by S-βGM (P = 0.11 with respect to Control) (**Figure 4**). Regarding lipid peroxidation, *Salmonella* Enteritidis significantly increased the production of conjugated dienes and secondary oxidation products (**Figure 5**). The addition of S-βGM in infected cultures did not significantly reduce the formation of conjugated dienes and secondary oxidations products (P = 0.07 and P = 0.20, respectively).

The results of cell-associated bacterial experiments (**Table 1**) indicated that S-βGM caused a significant reduction in intracellular *Salmonella* Enteritidis, although no effect on bacterial adhesion to Caco-2 cell cultures was detected (P = 0.30). Moreover, the data also indicated that S-βGM did not affect the viability of *Salmonella* Enteritidis (P = 0.80). Scanning and transmission microscopy images (**Supplemental Figure 1**) showed the capacity of S-βGM to agglutinate *Salmonella* Enteritidis to the surface of this product, which leads to a reduction in bacteria adhered to the epithelium as well as the formation of ruffles in an infected enterocyte.

In the case of *Salmonella* Dublin (**Table 2**), a MOI as low as 3 had the capacity to modify TER and D-mannitol flux. The highest MOI tested, 50, reduced TER and increased D-mannitol flux but also significantly increased LDH activity. For this reason, further experiments were performed with a MOI of 3. In these conditions, as for *Salmonella* Enteritidis, 500 μg/mL was the S-βGM concentration showing the highest protective effect, here again complete for TER (P = 0.80 respect to Control) and partial for D-mannitol flux. In the case of FD-4 flux, as in *Salmonella* Enteritidis infection, a lower effect was observed in comparison to the results obtained for D-mannitol (MOI of

3; 1.2-fold increase for FD-4 flux compared to 7.0-fold increase for D-mannitol flux). Moreover, a complete protective effect of S-βGM was observed (P = 0.46 respect to Control). Confocal images (**Supplemental Figure 2**) revealed similar results to those obtained for *Salmonella* Enteritidis.

Discussion

In a previous study, we found that S-βGM in chickens infected with *Salmonella* Enteritidis improved ZO-1 localization in the TJ (22), but we did not explore a possible direct interaction with intestinal epithelial cells in a model suitable for the study of epithelial barrier function. In the present study, however, we examined the effect of S-βGM in an *in vitro* model of intestinal Caco-2 cell culture, in which epithelial barrier function was disrupted by colonization with *Salmonella* Enteritidis and Dublin. Our results coincide with previous data suggesting a higher human pathogenic potential for *Salmonella* Dublin (24), since a lower MOI is sufficient to obtain similar effects on PP to those of *Salmonella* Enteritidis.

In the TJ, two routes have been reported to be involved in PP (29): a size-restrictive pore pathway permeable to small solutes and ions, and a non-restrictive leak pathway that regulates the flux of larger non-charged solutes, including macromolecules and bacterial antigens. Watson et al. (30) found that the size-restrictive pore pathway is normally present in mature Caco-2 cells and that the large-channel pathway is created in response to TJ-disrupting agents. TER measures the flux of small ions that do not discriminate between the pore and leak pathways (31). Similarly, D-mannitol, with a molecular radius of $4.1 \cdot 10^{-4}$ µm, is unsuitable for measuring TJ selectivity. However, FD-4, with a molecular radius of $1.4 \cdot 10^{-3}$ µm exclusively permeates the leak pathway

(32). In the case of *Salmonella* Typhimurium, several authors have described an increase in inulin and dextran fluxes, which are also considered to permeate the leak pathway (12, 13, 33). Therefore, the increase in FD-4 flux observed in the present study indicates the involvement of the leak pathway in *Salmonella* Enteritidis and Dublin infection. Interestingly, the total recovery induced by S-βGM in FD-4 flux suggests that this product reverses the effect of *salmonellae* on the leak pathway. Nevertheless, we cannot rule out the possibility that *salmonellae* also have an effect on size-restrictive pores since S-βGM did not completely reverse D-mannitol flux. In this respect, TNF-α, the main cytokine involved in s*almonellae* inflammatory effects (32) has been reported to increase permeability to both small and large molecules (34).

The loss of ZO-1 and occludin fluorescence in the TJ is a common feature also observed for *Salmonella* Typhimurium (12, 13, 35 36). We also observed the redistribution of ZO-1 in the intestine of chickens infected with *Salmonella* Enteritidis (22). As regards the presence of cytoplasmic occludin, this effect has also been reported in infection with *Salmonella* Typhimurium, and has been associated with protein dephosphorylation and redistribution from TJ to small cytoplasmic vesicles (13). Confocal images furthermore revealed the formation of stellate actin focal points of fluorescence in the convergence of several cells. Jepson et al. (37) attributed the formation of these structures to contraction of the perijunctional actomyosin ring in cells infected with *Salmonella* Typhimurium. In the case of *Salmonella* Enteritidis, La Ragione et al. (38) also observed cytoskeletal actin rearrangements induced by invading bacteria. The activation of tyrosine kinases has been implicated in actin rearrangements induced by *Salmonella* through the phosphorylation of several host proteins. Our results revealed that genistein prevented the effects of *Salmonella* Enteritidis on PP. Along the same lines, Wells et al.

(39) and Murli et al. (40) found that genistein reduces the invasion of *Salmonella* Typhimurium by a mechanism associated with the protection of perijunctional actin distribution. They also observed the capacity of genistein to reverse the effect of *Salmonella* Typhimurium on TER (39). Thus, we have corroborated the involvement of the perijunctional actin ring in *Salmonella* Enteritidis infection. Not all these changes in fluorescence distribution and quantification were completely reverted when the cultures where incubated with S-βGM. Similarly, Marchiendo et al. (41) reported that occludin accumulations remained elevated in the cytoplasm for a long period after the disruption of epithelial barrier function, thus providing an explanation for the absence of any recovery of occludin in our experimental conditions.

The mechanisms by which macrophages kill *Salmonella* via the production of ROS and reactive nitrogen species (RNS) are well described, as are the strategies employed by *Salmonella* to overcome oxidative stress (42). Nevertheless, there is little information concerning the generation of oxidative stress in infected enterocytes. Similar to our observations, Mehta et al. (43) observed that a cholera-like enterotoxin produced by *Salmonella* Typhimurium increases the production of conjugated dienes. In addition, we also found that the infection increases secondary oxidation products and intracellular ROS. In contrast, those authors found a correlation between oxidative stress and a reduction in cell viability, an effect that we did not observe since LDH activity was not modified in the range of MOIs tested. These results may indicate the involvement of oxidative stress in the TJ disruption induced by *Salmonella* Enteritidis. Moreover, it is interesting to note that oxidative stress also induces tyrosine phosphorylation of TJ proteins, causing the dissociation of occludin-ZO-1 complexes, and the dissociation of these complexes from cytoskeletal proteins (44). Therefore, oxidative stress seems to be

an important factor in the effects of *Salmonella* Enteritidis on epithelial barrier function; the reduction in ROS production in the presence of S-βGM may be responsible for the recovery of the epithelial barrier function, while the remaining cytoplasmic occludin accumulations may be related to the incomplete recovery of the control lipid peroxidation levels and D-mannitol flux exerted by this MOS.

In a previous study, we observed the capacity of S-βGM to reduce *Salmonella* Typhimurium adhesion to porcine intestinal epithelial cells (21). Our results in Caco-2 cells infected with *Salmonella* Enteritidis revealed that S-βGM did not affect bacterial adhesion, but did reduce epithelial invasion. One plausible explanation is that under these conditions, S-βGM remained adhered to the epithelium, and the bacteria adhered to the surface of S-βGM were counted as part of the adhesion. This difference may arise from differences in mannose receptors between Caco-2 and IPI-2I cells.

In summary, the capacity of S-βGM to modulate the leak pathway, reduce ROS production and agglutinate bacteria contributes to its protective effect on epithelial barrier function. This capacity is clearly demonstrated in the Caco-2 cell model described here, in which a direct effect on PP was observed. Moreover, this product also reduces the number of M cells, increases the production of mucus, and modulates the immune response (21, 22). In conclusion, our data provide further evidence of the positive effects of the inclusion of this product in animal nutrition and of its benefits for human consumers.

Acknowledgements

We gratefully acknowledge I. Badiola (CReSA, IRTA-UAB) for providing the *Salmonella* Enteritidis and Dublin strains and Language Services of the *Universitat de Barcelona* for language assistance. The authors are indebted to the staff of the *Centres Científics i Tecnològics* of the *Universitat de Barcelona*.

SC, JB, BV, FG, RF and RMV designed research; MTB, JCS, RB and AMM conducted research; MTB analyzed data; MTB, RF and RMV wrote the paper. MTB, RF and RMV had primary responsibility for final content. All authors read and approved the final manuscript.

References

1. European Food Safety Authority. The European Union Summary Report on Trends and Sources of Zoonoses, Zoonotic Agents and Food-borne Outbreaks in 2014. EFSA Journal. 2015;13:4329. http://www.efsa.europa.eu/en/efsajournal/pub/4329
2. De Buck JF, Van Immerseel F, Haesebrouck F, Ducatelle R. Colonization of the chicken reproductive tract and egg contamination by Salmonella. J Appl Mircobiol. 2004;97:233-245.
3. Marcus R, Rabatsky-Ehr T, Mohle-Boetani JC, Farley M, Medus C, Shiferaw B, Carter M, Zansky S, Kennedy M, Van Gilder T, Hadler JL; Emerging Infections Program FoodNet Working Group. Dramatic decrease in the incidence of Salmonella serotype Enteritidis infections in 5 FoodNet sites: 1996-1999. Clin Infect Dis. 2004;38:S135-S141.
4. Patrick ME, Adcock PM, Gomez TM, Altekruse SF, Holland BH, Tauxe RV, Swerdlow DL. Salmonella enteritidis infections, United States, 1985-1999. Emerg Infect Dis. 2004;10:1-7.
5. Little CL, Rhoades JR, Hucklesby L, Greenwood M, Surman-Lee S, Bolton FJ, Meldrum R, Wilson I, McDonald C, de Pinna E, Threlfall EJ, ChanCH. Survey of Salmonella contamination of raw shell eggs used in food service premises in the United Kingdom, 2005 through 2006. J Food Prot. 2008;71:19-26.
6. Lister SA. Salmonella Enteritidis infection in broilers and broiler breeders. Vet Rec. 1988;123:350.
7. Velge P, Cloeckaert A, Barrow P. Emergence of Salmonella epidemics: the problems related to Salmonella enterica serotype Enteritidis and multiple antibiotic resistance in other major serotypes. Vet Res. 2005;36:267-288.

8. Golden NJ, Marks HH, Coleman ME, Schroeder CM, Bauer NE Jr, Schlosser WD. Review of induced molting by feed removal and contamination of eggs with Salmonella enterica serovar Enteritidis. Vet Microbiol. 2008;131:215-228.
9. Spring, P., Wenk, C., Dawson, K.A. i Newman K.E. The effects of dietary mannan oligosaccharides on cecal parameters and the concentrations of enteric bacteria in the cecae of Salmonella-challenged broiler chicks. Poult Sci. 2000;79:205-211.
10. Santos RL, Bäumler AJ. Cell tropism of Salmonella enterica. Int J Med Microbiol. 2004;294:225-233.
11. Broz P, Ohlson MB, Monack DM. Innate immune response to Salmonella typhimurium, a model enteric pathogen. Gut Microbes. 2012;3:62-70.
12. Tafazoli F, Magnusson KE, Zheng L. Disruption of epithelial barrier integrity by Salmonella enterica serovar typhimurium requires geranylgeranylated proteins. Infect Immun. 2003;71:872-881.
13. Köhler H, Sakaguchi T, Hurley BP, Kase BJ, Reinecker HC, McCormick BA. Salmonella enterica serovar Typhimurium regulates intercellular junction proteins and facilitates transepithelial neutrophil and bacterial passage. Am J Physiol Gastrointest Liver Physiol. 2007;293:G178-G187.
14. Miyoshi J, Takai Y. Structural and functional associations of apical junctions with cytoskeleton. Biochim Biophys Acta. 2008;1778:670-691.
15. Suzuki T. Regulation of intestinal epithelial permeability by tight junctions. Cell. Mol. Life Sci. 2013;70:631–659.
16. Gaggìa F, Mattaelli P, Biavatti. Probiotics and prebiotics in animal feeding for sale food production. Int J Food Mircobiol. 2010;141:S15-S28.

17. Hooge DM. Meta-analysis of Broiler chicken pen trials evaluating dietary mannan oligosaccharide, 1993-2003. Int. J. Poult. Sci. 2004;3:163-174.
18. Kogan G, Kocher A. Role of yeast cell wall polysaccharides in pig nutrition and health protection. Livest Sci. 2007;109:161-165.
19. Iji PA, Saki AA, Tivey DR. Intestinal structure and function of broiler chickens on diets supplemented with a mannan oligosaccharide. J Sci Food Agric. 2001;81:1186-1192.
20. Ferket PR, Parks CW, Grimes JL. Benefits of dietary antibiotic and mannanoligosaccharide supplementation for poultry. In: Proc. Multi-State. Meet., Indianapolis, 2002. IN. p. 63-76.
21. Badia R, Brufau MT, Guerrero-Zamora AM, Lizardo R, Dobrescu I, Martin-Venegas R, Ferrer R, Salmon H, Martínez P, Brufau J. β-Galactomannan and Saccharomyces cerevisiae var. boulardii modulate the immune response against Salmonella enterica serovar Typhimurium in porcine intestinal epithelial and dendritic cells. Clin Vaccine Immunol. 2012;19:368-376.
22. Brufau MT, Martín-Venegas R, Guerrero-Zamora AM, Pérez-Vendrell AM. Vilà B, Brufau J, Ferrer R. Dietary β-galactomannans have beneficial effects on the intestinal morphology of chickens challenged with Salmonella enterica serovar Enteritidis. J Anim Sci. 2015;93:238-246.
23. Rao R. Oxidative stress-induced disruption of epithelial and endothelial tight junction. Front Biosc. 2008;13:7210-7226.
24. European Food Safety Authority. Quantitative estimation of the impact of setting a new target for the reduction of Salmonella in breeding hens of Gallus gallus. 2009. http://www.efsa.europa.eu/en/efsajournal/pub/1036

25. Martín-Venegas R, Brufau MT, Guerrero-Zamora AM, Mercier Y, Geraert PA, Ferrer R. The methionine precursor DL-2-hydroxy-(4-methylthio)butanoic acid protects intestinal epithelial barrier function. Food Chem. 2013;141:1702-1709.
26. Martín-Venegas R, Brufau MT, Mañas-Cano O, Mercier Y, Nonis MK, Ferrer R. Monocarboxylate transporter 1 is up-regulated in Caco-2 cells by the methionine precursor DL-2-hydroxy-(4-methylthio)butanoic acid. Vet J. 2014;202:555-560.
27. Roig-Pérez S, Cortadellas N, Moretó M, Ferrer R. Intracellular mechanisms involved in docosahexaenoic acid-induced increases in tight junction permeability in Caco-2 cell monolayers. J Nutr. 2010;140:1557-1563.
28. Peterson, G. Evaluation of the biochemical targets of genistein in tumor cells. J. Nutr.1995;125:784S–789S.
29. Van Itallie CM, Holmes J, Bridges A, Gookin JL, Coccaro MR, Proctor W, Colegio OR, Anderson JM. The density of small tight junction pores varies among cell types and is increased by expression of claudin-2. J Cell Sci. 2008;121:298-305.
30. Watson CJ, Rowland M, Warhurst G. Functional modeling of tight junctions in intestinal cell monolayers using polyethylene glycol oligomers. Am J Physiol Cell Physiol. 2001;281:C388-C397.
31. Shen L, Weber CR, Raleigh DR, Yu D, Turner JR. Tight junction pore and leak pathways: a dynamic duo. Annu Rev Physiol. 2011;73:283-309.
32. Al-Sadi R, Khatib K, Guo S, Ye D, Youssef M, Ma T. Occludin regulates macromolecule flux across the intestinal epithelial tight junction barrier. Am J Physiol Gastrointest. Liver Physiol. 2011;300:G1054-G1064.

33. Jepson MA, Schlecht HB, Collares-Buzato CB. Localization of dysfunctional tight junctions in Salmonella enterica serovar typhimurium-infected epithelial layers. Infect Immun. 2000;68:7202-7208.

34. Cunningham KE, Turner JR. Myosin light chain kinase: pulling the strings of epithelial tight junction function. Ann N Y Acad Sci. 2012;1258:34-42

35. Bertelsen LS, Paesold G, Marcus SL, Finaly BB, Eckmanm L, Barrett KE. Modulation of chloride secretory responses and barrier function of intestinal epithelial cells by the Salmonella effector protein SigD. Am J Physiol Cell Physiol. 2004;287:C939-C948.

36. Yu Q, Zhu L, Wang Z, Li P, Yang Q. Lactobacillus delbrueckii ssp. lactis R4 prevents Salmonella typhimurium SL1344-induced damage to tight junctions and adherens junctions. J Microbiol. 2012;50:613-617.

37. Jepson MA, Collares-Buzato CB, Clark MA, Hirst BH, Simmons NL. Rapid disruption of epithelial barrier function by Salmonella typhimurium is associated with structural modification of intercellular junctions. Infect Immun. 1995;63:356-359.

38. La Ragione RM, Cooley WA, Velge P, Jepson MA, Woodward MJ. Membrane ruffling and invasion of human and avian cell lines is reduced for aflagellate mutants of Salmonella enterica serotype Enteritidis. Int J Med Microbiol. 2003;293:261-272.

39. Wells CL, Jechorek RP, Kinneberg KM, Debol SM, Erlandsen SL. The isoflavone genistein inhibits internalization of enteric bacteria by cultured Caco-2 and HT-29 enterocytes. J Nutr. 1999;129:634-640.

40. Murli S, Watson RO, Galán JE. Role of tyrosine kinases and the tyrosine phosphatase SptP in the interaction of Salmonella with host cells. Cell Microbiol. 2001;3:795-810.
41. Marchiando AM, Shen L, Graham WV, Weber CR, Schwarz BT, Austin JR 2nd, Raleigh DR, Guan Y, Watson AJ, Montrose MH, Turner JR. Caveolin-1-dependent occludin endocytosis is required for TNF-induced tight junction regulation in vivo. J Cell Biol. 2010;189:111-126.
42. Babu US, Gaines DW, Lillehoj H, Raybourne RB. Differential reactive oxygen and nitrogen production and clearance of Salmonella serovars by chicken and mouse macrophages. Dev Comp Immunol. 2006;30:942-953.
43. Mehta A, Singh S, Ganguly NK. Effect of Salmonella typhimurium enterotoxin (S-LT) on lipid peroxidation and cell viability levels of isolated rat enterocytes. Mol Cell Biochem. 1999;196:175-181.
44. Rao RK, Basuroy S, Rao VU, Karnaky Jr KJ, Gupta A. Tyrosine phosphorylation and dissociation of occludin-ZO-1 and E-cadherin-beta-catenin complexes from the cytoskeleton by oxidative stress. Biochem J. 2002;368:471-481.

Table 1. Effect of S-βGM on Caco-2 cell invasion and adhesion and *Salmonella* Enteritidis viability.

	SE	SE + S-βGM
Invasion ($CFU \cdot 10^5/mL$)[1]	34 ± 3.5	23 ± 2.7*
Adhesion ($CFU \cdot 10^5/mL$)[1]	90 ± 7.1	111 ± 18.2
Viability ($CFU \cdot 10^4/mL$)[2]	86 ± 9.2	89 ± 6.5

[1]Caco-2 cells were incubated for 3 h in the presence of *Salmonella* Enteritidis MOI 10 or *Salmonella* Enteritidis plus S-βGM (500 μg/mL). [2]*Salmonella* Enteritidis was incubated for 3 h in the absence or presence of S-βGM (500 μg/mL). Results are expressed as the mean ± SEM of $n = 4$ experiments. *Differ from SE, $P < 0.05$ (Student's t test). MOI, multiplicity of infection; S-βGM, Salmosan®; SE, *Salmonella* Enteritidis.

Table 2. Effect of S-βGM on epithelial barrier function and viability of Caco-2 cells infected with *Salmonella* Dublin[1].

	LDH (Abs)	TER ($\Omega \cdot cm^2 \cdot 10^3$)	D-mannitol flux (fmol/cm²)	FD-4 flux (FI)
Control	0.32 ± 0.0030[b]	2.26 ± 0.0514[a]	4.0 ± 0.32[d]	0.54 ± 0.036[a,b]
MOI 3	0.33 ± 0.0047[b]	1.50 ± 0.0815[b]	28.4 ± 2.52[b]	0.64 ± 0.041[a]
MOI 5	0.33 ± 0.0036[b]	1.43 ± 0.109[b]	22.1 ± 2.25[b]	ND
MOI 10	0.33 ± 0.0034[b]	1.55 ± 0.0619[b]	21.1 ± 1.72[b]	ND
MOI 50	0.35 ± 0.0046[a]	0.858 ± 0.0674[c]	41.8 ± 1.70[a]	ND
MOI 3 + S-βGM	0.32 ± 0.0049[b]	2.22 ± 0.0873[a]	19.3 ± 2.14[c]	0.51 ± 0.029[b]

[1]Cultures were incubated for 3 h in the absence (Control) or presence of *Salmonella* Dublin (from MOI 3 to 50) and *Salmonella* Dublin plus S-βGM (500 µg/mL). Results are expressed as the mean ± SEM of n = 12 monolayers. Labeled means in a column without a common letter differ, $P < 0.05$ (post hoc Bonferroni test). Abs, Absorbance; FD-4, fluorescein isothiocyanate–dextran; FI, intensity of fluorescence; LDH, lactate dehydrogenase; MOI, multiplicity of infection; ND, not determined; S-βGM, Salmosan®; TER, transepithelial electrical resistance.

Figure legends

Figure 1. TER and D-mannitol flux in Caco-2 infected with *Salmonella* Enteritidis at different MOIs. Cultures were incubated for 3 h in the absence (Control) or presence of increasing MOIs of *Salmonella* Enteritidis (from MOI 3 to 50). Results are expressed as the mean ± SEM of n = 9 monolayers. * Different from Control, $P < 0.05$ (post hoc Dunnett test). MOI, multiplicity of infection; TER, transepithelial electrical resistance.

Figure 2. Protective role of S-βGM on epithelial barrier function in Caco-2 cells infected with *Salmonella* Enteritidis. TER (A), D-mannitol flux (B) and FD-4 flux (C) in cultures incubated for 3 h in the absence (Control) or presence of *Salmonella* Enteritidis (MOI 10) and *Salmonella* Enteritidis plus S-βGM (500 µg/mL) or genistein (300 µM). Results are expressed as the mean ± SEM of n = 15 monolayers for TER and D-mannitol flux and n = 12 for FD-4 flux. Labeled means without a common letter differ, $P < 0.05$ (post hoc Bonferroni test). FD-4, fluorescein isothiocyanate–dextran; FI, intensity of fluorescence; MOI, multiplicity of infection; S-βGM, Salmosan®; SE, *Salmonella* Enteritidis; TER, transepithelial electrical resistance.

Figure 3. Recovery of TJ protein localization by S-βGM in Caco-2 cells infected with *Salmonella* Enteritidis. Occludin, ZO-1 and actin confocal images (A) and intensity of fluorescence calculated from these images (B) in cultures incubated for 3 h in the absence (Control) or presence of *Salmonella* Enteritidis (MOI 10) and *Salmonella* Enteritidis plus S-βGM (500 µg/mL). The results shown are representative of 3 experiments. FI, intensity of fluorescence; MOI, multiplicity of infection; S-βGM, Salmosan®; SE, *Salmonella* Enteritidis; ZO-1, zonula occludens protein-1.

Figure 4. S-βGM reduces ROS production in Caco-2 cells infected with *Salmonella* Enteritidis. Cultures were incubated for 3 h in the absence (Control) or presence of *Salmonella* Enteritidis (MOI 10) and *Salmonella* Enteritidis plus S-βGM (500 µg/mL). H_2O_2 (1 mmol/L) was used as positive Control. Results are expressed as FI = (FI_{3h}-FI_{0h})/FI_{0h} x 100, as the mean ± SEM of n = 12 monolayers. Labeled means without a common letter differ, $P < 0.05$ (post hoc Bonferroni test). FI, intensity of fluorescence; MOI, multiplicity of infection; ROS, reactive oxygen species; S-βGM, Salmosan®; SE, *Salmonella* Enteritidis.

Figure 5. Effect of S-βGM on lipid peroxidation in Caco-2 cells infected with *Salmonella* Enteritidis. Cultures were incubated for 3 h in the absence (Control) or presence of *Salmonella* Enteritidis (MOI 10) and *Salmonella* Enteritidis plus S-βGM (500 µg/mL). Absorbance at 235 nm was mainly attributed to conjugated dienes and 270 nm, to secondary oxidation products. Results are expressed as absorbance normalized by cell number, as the mean ± SEM of n = 8 experiments (each experiment consisted of 4 monolayers for each condition). For each series, labeled means without a common letter differ, $P < 0.05$ (post hoc Bonferroni test). Abs, Absorbance; MOI, multiplicity of infection; S-βGM, Salmosan®; SE, *Salmonella* Enteritidis.

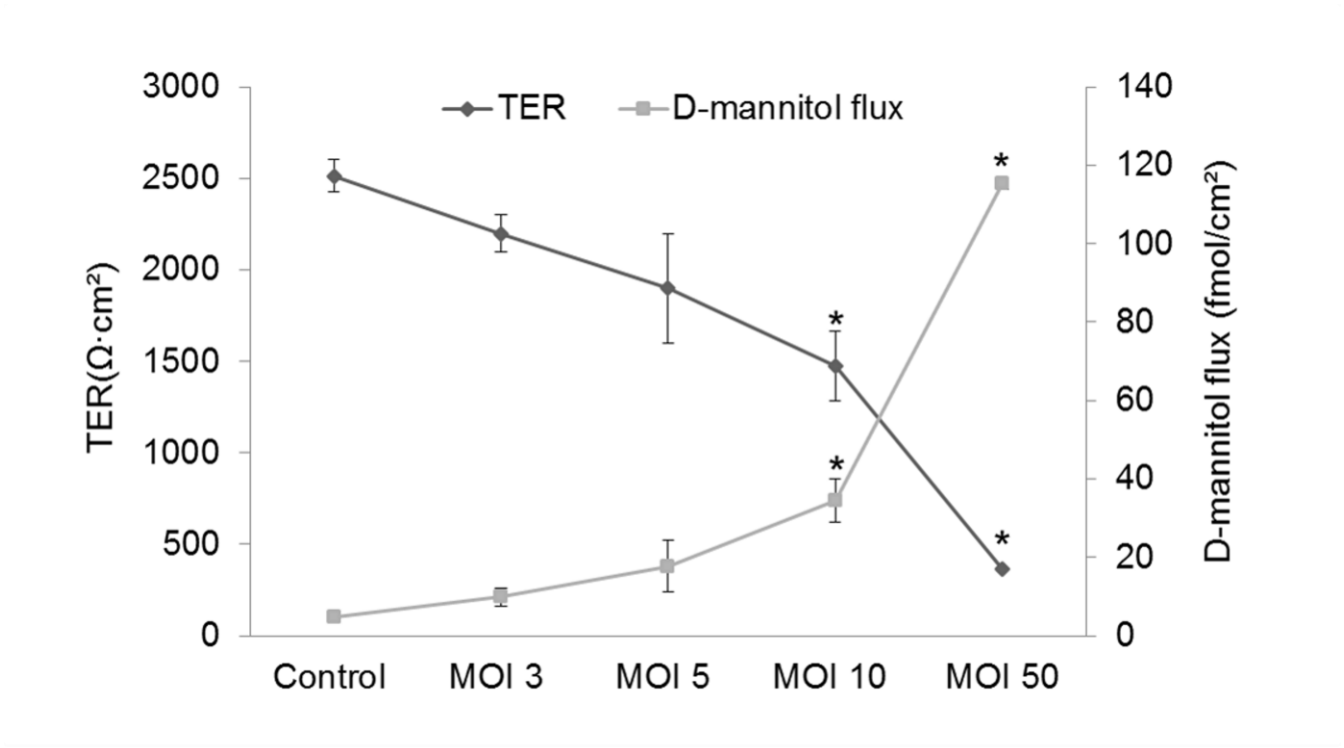
TER
D-mannitol flux
TER(Ω·cm²)
D-mannitol flux (fmol/cm²)
3000
2500
2000
1500
1000
500
0
140
120
100
80
60
40
20
0
*
*
*
*
Control
MOI 3
MOI 5
MOI 10
MOI 50

Fig. 1

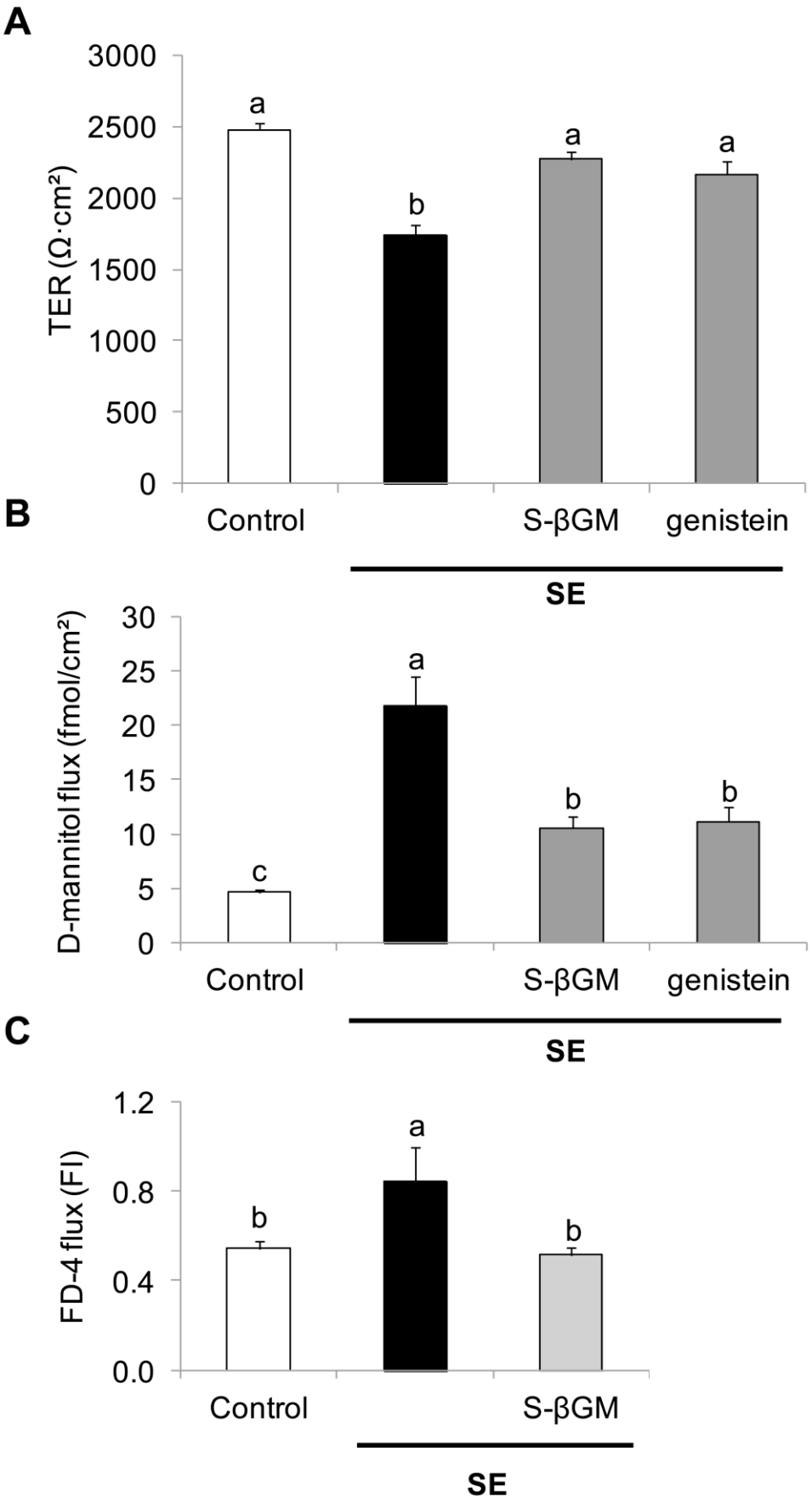
A
3000
2500
2000
1500
1000
500
0
TER (Ω·cm²)
a
b
a
a
Control
S-βGM
genistein
SE
B
30
25
20
15
10
5
0
D-mannitol flux (fmol/cm²)
c
a
b
b
Control
S-βGM
genistein
SE
C
1.2
0.8
0.4
0.0
FD-4 flux (FI)
b
a
b
Control
S-βGM
SE

Fig. 2

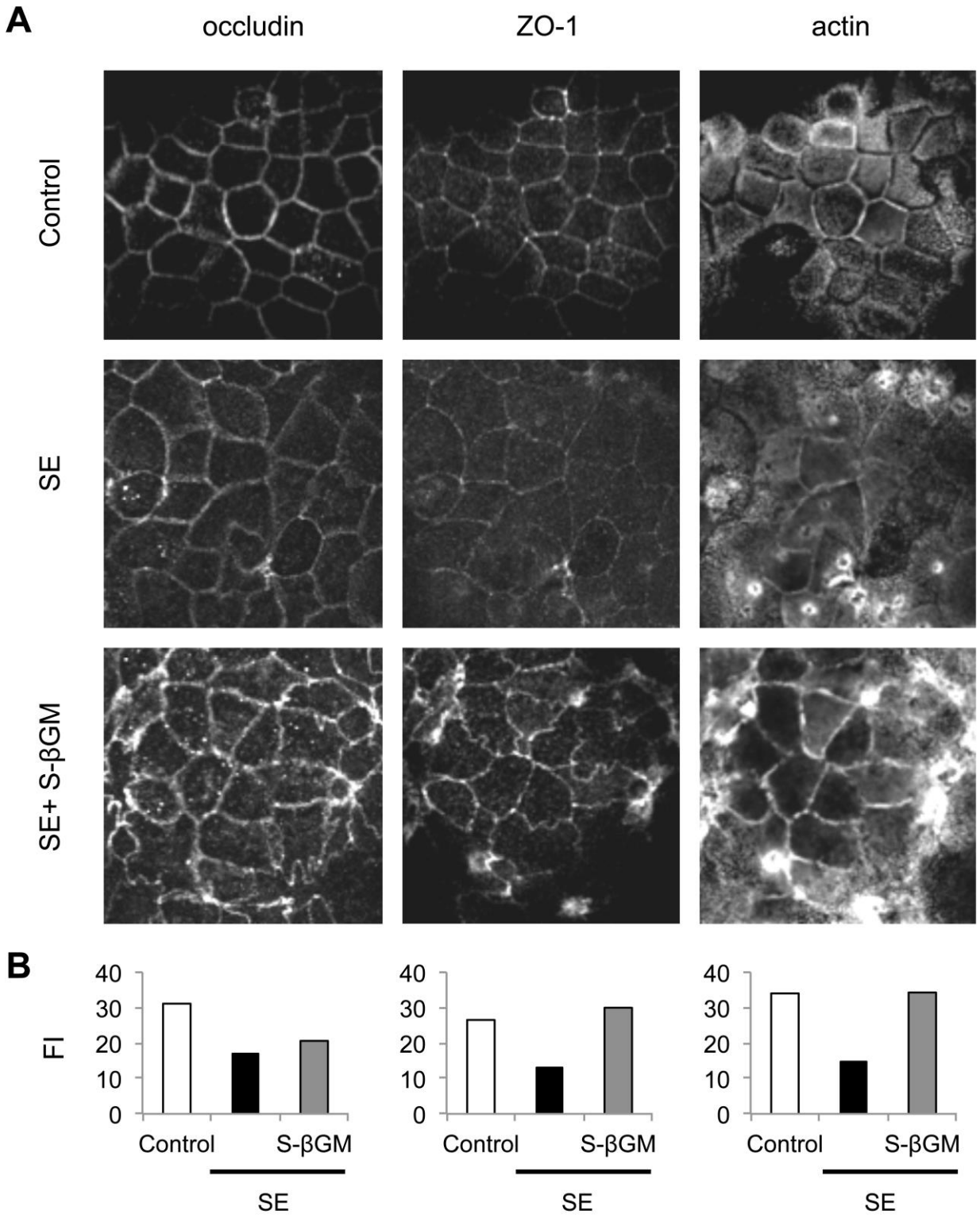
A
occludin
ZO-1
actin
Control
SE
SE+ S-βGM
B
FI
40
30
20
10
0
Control
S-βGM
SE

Fig. 3

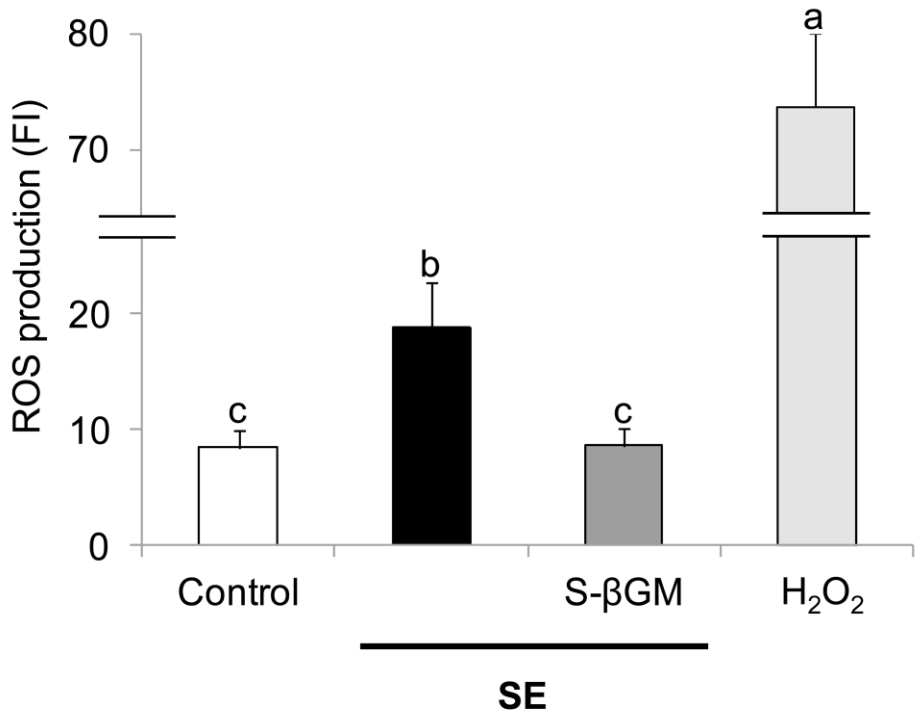
ROS production (FI)
80
70
20
10
0
a
b
c
c
Control
S-βGM
H2O2
SE

Fig. 4

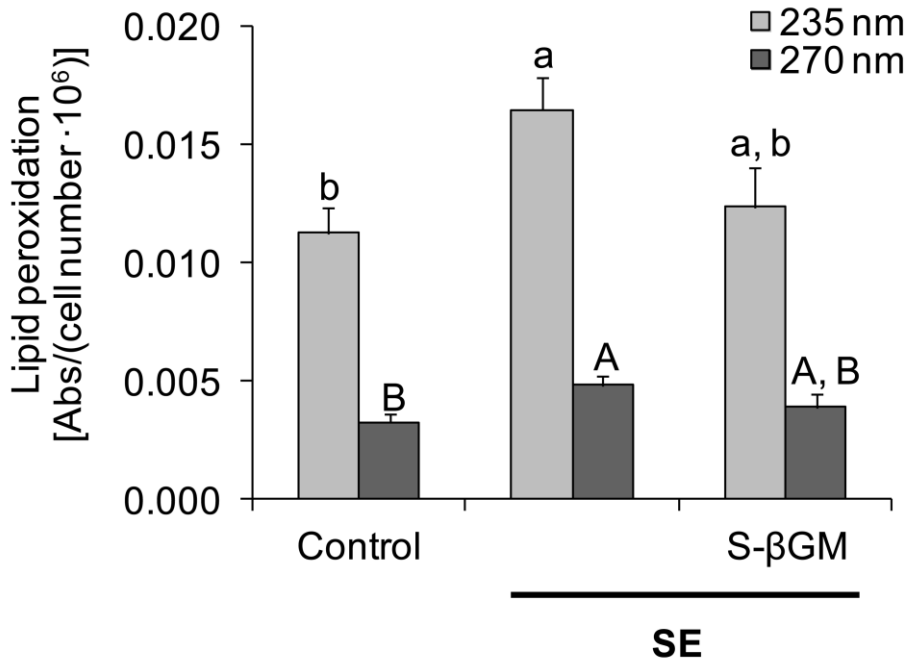
Lipid peroxidation
[Abs/(cell number ·10^6)]
0.020
0.015
0.010
0.005
0.000
235 nm
270 nm
a
b
a, b
A
B
A, B
Control
S-βGM
SE

Fig. 5

Online Supporting Material

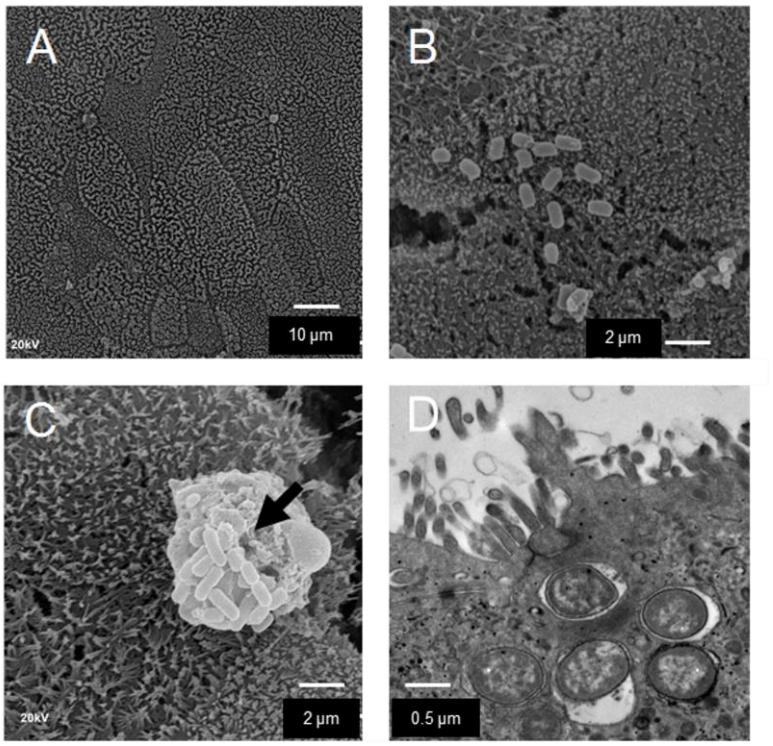

Supplemental Figure 1. S-βGM agglutinates *Salmonella* Enteritidis in Caco-2 cell cultures. Scanning (A-C) and transmission electron microscopy images (D) of cultures incubated for 3 h in the absence (A, Control) or presence of *Salmonella* Enteritidis (B and D, MOI 10) and *Salmonella* Enteritidis plus 500 µg/mL S-βGM (C). The arrow indicates bacteria attached to the surface of the product. The images are representative of 3 experiments. MOI, multiplicity of infection; S-βGM, Salmosan®.

Online Supporting Material

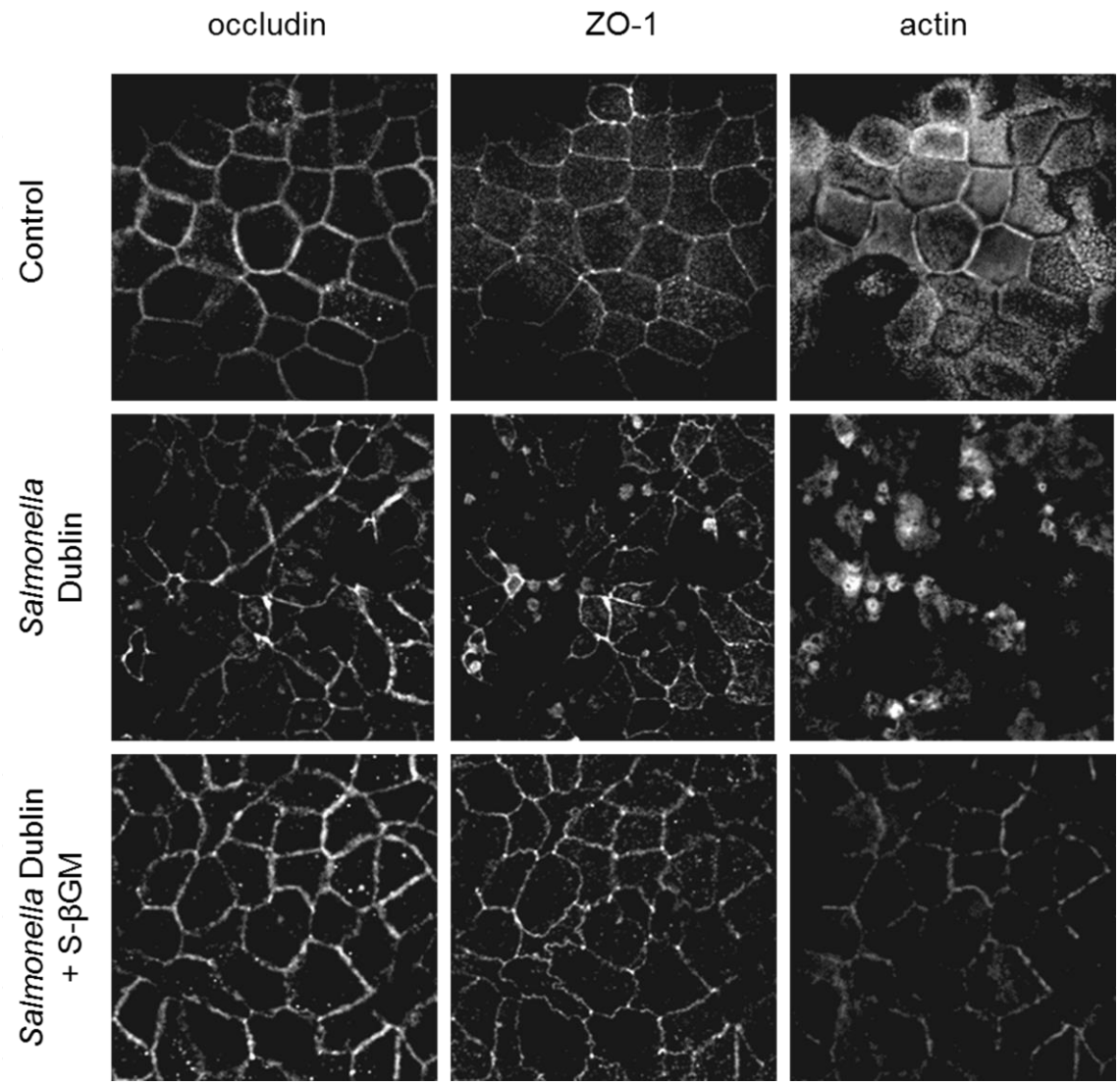

Supplemental Figure 2. Recovery of TJ protein localization by S-βGM in Caco-2 cells infected with *Salmonella* Dublin. Immunofluorescence images of occludin, ZO-1 and actin in cultures incubated for 3 h in the absence (Control) or presence of *Salmonella* Dublin (MOI 3) and *Salmonella* Dublin plus S-βGM (500 μg/mL). The results shown are representative of 3 experiments. MOI, multiplicity of infection; S-βGM, Salmosan®; ZO-1, zonula occludens protein-1.